ADVANCED SIMULATIONS OF OPTICAL TRANSITION AND DIFFRACTION RADIATION

T. Aumeyr[1], M. G. Billing[2], L.M. Bobb[1,3], B. Bolzon[3,4,5], E. Bravin[3], P. Karataev[1], K. Kruchinin[1], T. Lefevre[3] and S. Mazzoni[3]

1. John Adams Institute at Royal Holloway, Egham UK
2. CLASSE, Cornell University, Ithaca, USA
3. CERN, European Organisation for Nuclear Research, Geneva, Switzerland
4. Cockcroft Institute, Daresbury, Warrington, UK
5. University of Liverpool, UK

Overview

- Introduction
- What is Zemax?
- What is simulated and how does it work?
- Comparison with analytical theory
- Misalignments and error study
- Comparison with experimental results
- Conclusions

Introduction

- Next generation LC (CLIC, ILC) and also X-Ray FELs require transverse beam size measurements with µm resolution:
  - Wire scanner: disturbs the beam; can be destroyed by high intensity beams.
  - Laser-wire: non-invasive high resolution measurements; many are required over long distances (cost, maintenance)
- OTR: charged particle crosses a boundary between two media with different dielectric properties
  - Widely used for transverse profile measurements
  - OTR monitors: simple, robust and give direct image of 2D beam profile
  - OTR PSF structure: extract beam size with sub-µm resolution
  - Invasive method: degrade beam properties or beam can destroy target → diagnose low intensity pilot beams
- ODR: charged particle moves in the vicinity of a medium.
  - Spatial-spectral properties are sensitive to various beam parameters.
  - Energy loss due very small, beam parameters are unchanged → non-invasive diagnostics

Zemax

- Readily available commercial optical design software: standard tool to conceptualise, design, optimise, analyse and tolerance optical systems.
- Geometrical ray tracing is incomplete description of light propagation.
- Coherent process: wavefront travels through free space and interferes with itself → physical optics.
- Physical Optics Propagation (POP): Zemax mode that calculates wavefront propagation through an optical system surface by surface.
- Target as radiation source: initial electric field defined in 2D matrix (binary or text) or computed with Windows Dynamic Link Library (DLL).
- In POP: wavefront modelled with this array (dimension, sampling and aspect ratio are user-definable).
- Array then propagated in free space between optical surfaces → transfer function is computed at each surface → matrix is propagated from one side to the other.
- In this way, simulation of any source of light is possible (e.g. TR, DR, synchrotron radiation (SR)).

Electric source field

Y-polarisation component electric field for the induced by a single electron on a target surface [1]:

$$\Re\left\{E_y\right\} = \frac{2e}{\gamma\lambda\cos\theta_0}\left\{\frac{y}{\rho}K_1\left[\frac{2\pi}{\beta\gamma\lambda}\rho\right]\cos\phi\cos\theta_0 + \frac{1}{\gamma}K_0\left[\frac{2\pi}{\beta\gamma\lambda}\rho\right]\sin\phi\sin\theta_0\right\}$$

$$\Im\left\{E_y\right\} = \frac{2e}{\gamma\lambda\cos\theta_0}\left\{\frac{y}{\rho}K_1\left[\frac{2\pi}{\beta\gamma\lambda}\rho\right]\sin\phi\cos\theta_0 - \frac{1}{\gamma}K_0\left[\frac{2\pi}{\beta\gamma\lambda}\rho\right]\cos\phi\sin\theta_0\right\}$$

with $\beta = \sqrt{1 - \frac{1}{\gamma^2}}$, phase shift $\phi = ky\tan\theta_0\left(1 - \frac{1}{\beta}\right)$, $k = \frac{2\pi}{\lambda}$ and $\rho = \sqrt{x^2 + y^2}$.

x and *y* are two orthogonal coordinates of the target measured from the point of electron incidence, *γ* is the charged particle Lorentz factor, *λ* is the radiation wavelength, θ_0 is the angle between the trajectory of the particle and the screen plane, K_0 and K_1 are the zeroth and first order modified Bessel function. For TR, the entire field is propagated towards the observation plane.

[1] D. V. Karlovets and A. P. Potylitsyn, Nucl. Instrum. Meth. B266, 3738 (2008).

Transition Radiation
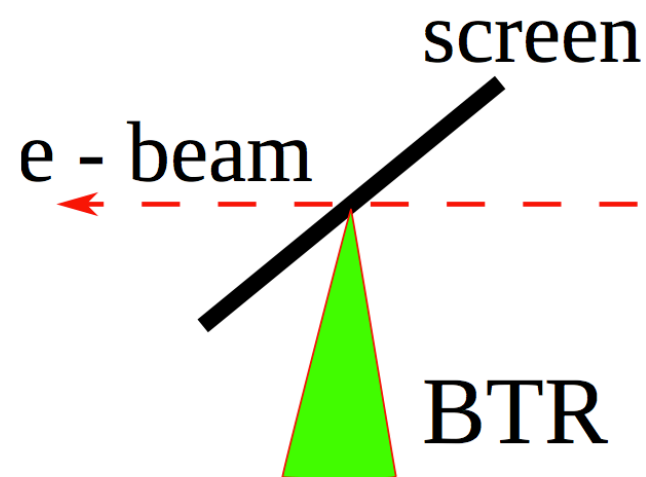
- Transition radiation (TR) appears when a charged particle crosses a boundary between two media with different dielectric constants

- The resolution is determined by the source dimensions induced by a single particle plus distortion caused by the optical system (diffraction of OTR tails, aberrations)

TR – free space propagation

- Demonstrate the validity of the simulation method: compare far-field simulations with well-known analytical theory.

- Angular distribution of intensity in the far-field of a charged particle passing through a boundary between vacuum and an ideal conductor with ultra-relativistic approximation (θ_x, θ_y, $\gamma^{-1} \ll 1$) [2]

$$\frac{d^2W_y^{TR}}{d\omega d\Omega} = \frac{\alpha}{\pi^2} \frac{\theta_y^{\,2}}{\left(\gamma^{-2} + \theta_x^{\,2} + \theta_y^{\,2}\right)^2} \frac{1}{\left(1 - \theta_y \cot\theta_0\right)^2}$$

[2] A. P. Potylitsyn, Nucl. Instrum. Meth. B145, 169 (1998).

Far field

$$L \gg \frac{\gamma^2 \lambda}{2\pi}$$
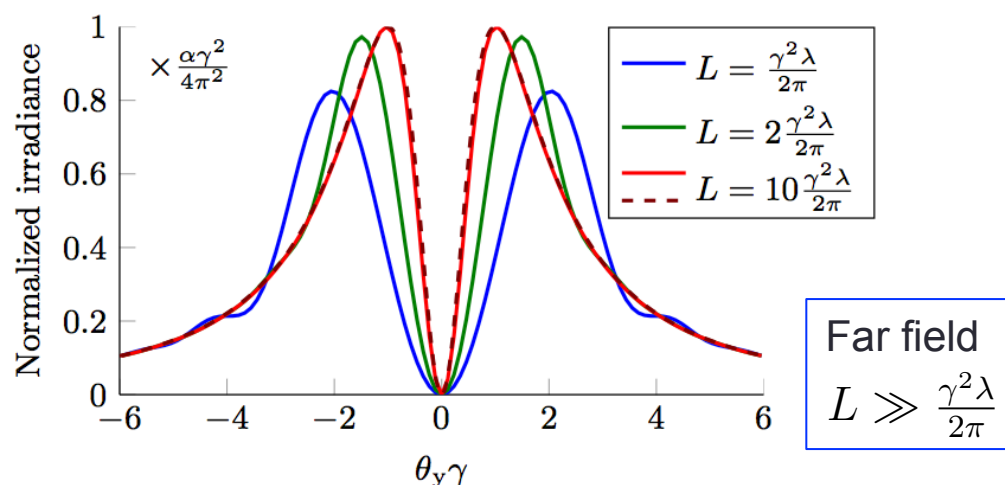
FIG. 2. Comparison between theoretical (dashed) and simulated (solid) TR angular distribution for various distances between source and image plane L ($\lambda = 550$ nm, $\gamma = 2500$, $\theta_x = 0$).
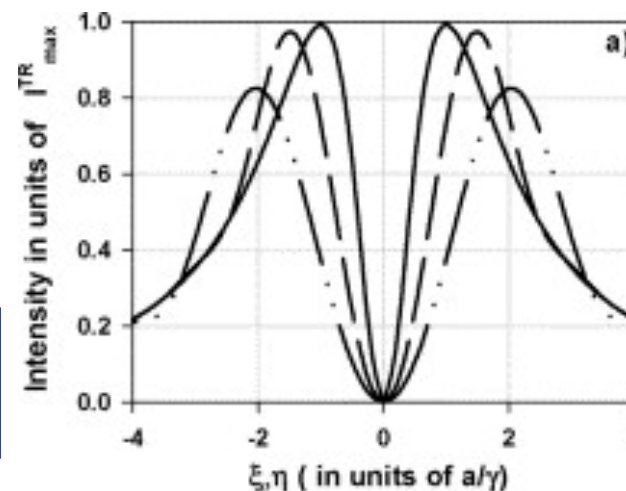
[3] P. V. Karataev, Phys. Lett. A 345, 428 (2005).

TR – free space propagation, tilted target

- Angular distribution of intensity in the far-field of a charged particle passing through a boundary between vacuum and an ideal conductor with ultra-relativistic approximation (θ_x, θ_y, γ^{-1} << 1) [2]

$$\frac{d^2 W_y^{TR}}{d\omega d\Omega} = \frac{\alpha}{\pi^2} \frac{\theta_y^2}{\left(\gamma^{-2} + \theta_x^2 + \theta_y^2\right)^2} \frac{1}{\left(1 - \theta_y \cot \theta_0\right)^2}$$

[2] A. P. Potylitsyn, Nucl. Instrum. Meth. B145, 169 (1998).
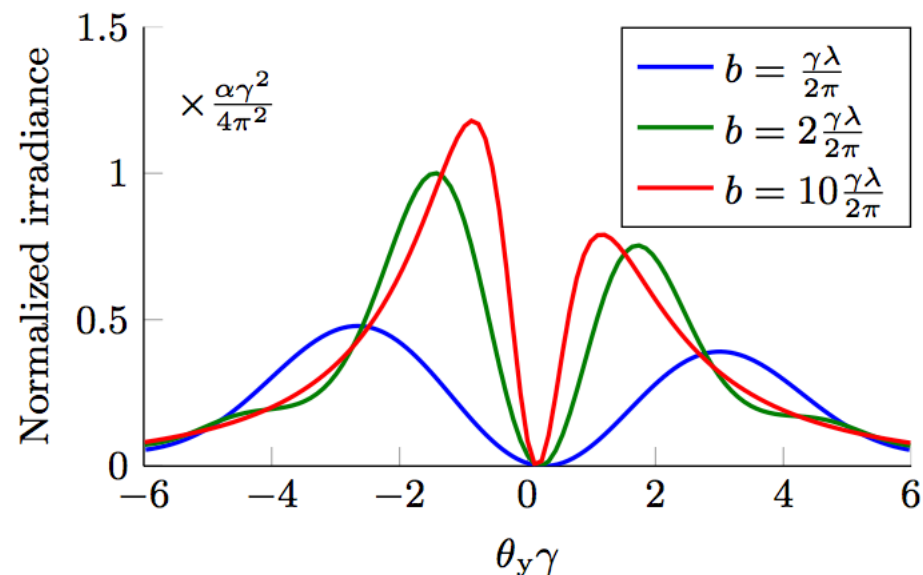
FIG. 3. TR angular distribution in the far-field using a tilted screen and for various target disc radii b ($\lambda = 550$ nm, $\gamma = 10$, $\theta_x = 0$, $\theta_0 = 45°$).

OTR PSF

- Resolution of optical TR (OTR) monitors is normally defined as a root-mean-square of the so-called point spread function (PSF). The OTR PSF has a structure itself which can be used to extract the beam size with sub-μm resolution resolution.

- To study the PSF, the simulated detector plane has to be in the image plane of a lens.
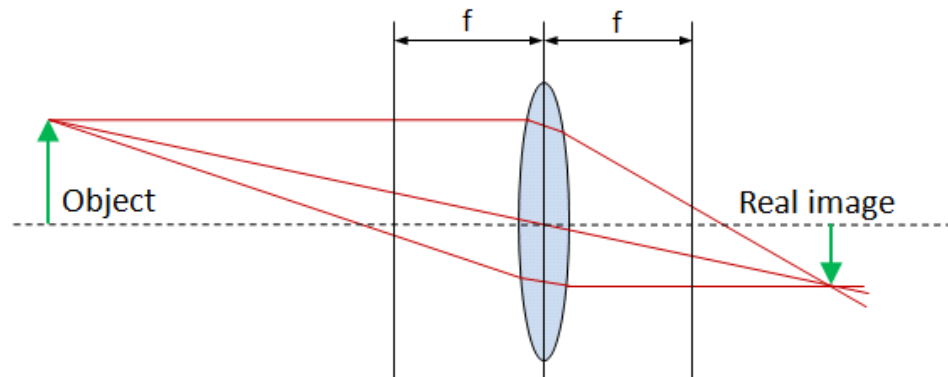
- The power of the ZEMAX tool is that any optical system can be built and nominally adjusted to a real one by using exact commercial products.

OTR PSF – misalignments

- The PSF is highly sensitive to misalignment: asymmetry is growing when increasing the horizontal lens offset.

- Displacing the lens longitudinally causes the PSF to broaden: minimum peak separation achieved at the image plane.
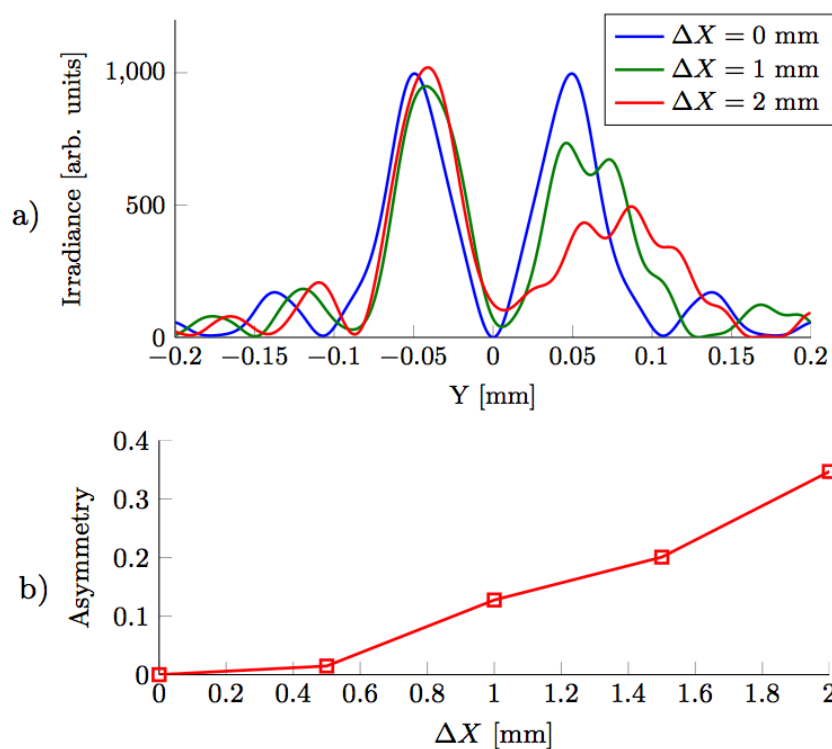
FIG. 5. TR PSF (a) and asymmetry (b) for various horizontal lens offsets ΔX ($\lambda = 550$ nm, $\gamma = 2500$, $\theta_x = 0$, $M = -7.4$).
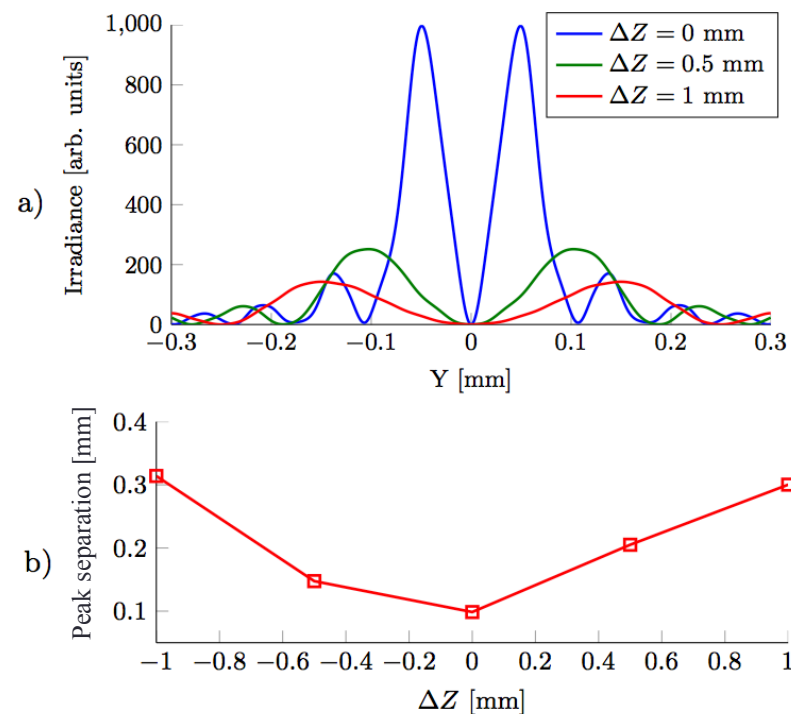
FIG. 6. TR PSF (a) and distance between the two main lobes (b) for various longitudinal lens offsets ΔZ ($\lambda = 550$ nm, $\gamma = 2500$, $\theta_x = 0$, $M = -7.4$).

OTR PSF – lens size

- Diffraction with a too small lens: diffraction is reduced when increasing the lens diameter → peak separation decreases until the introduction of aberrations increases the peak distance again.

- The peak separation remains constant as soon as the entire OTR light is captured by the lens.
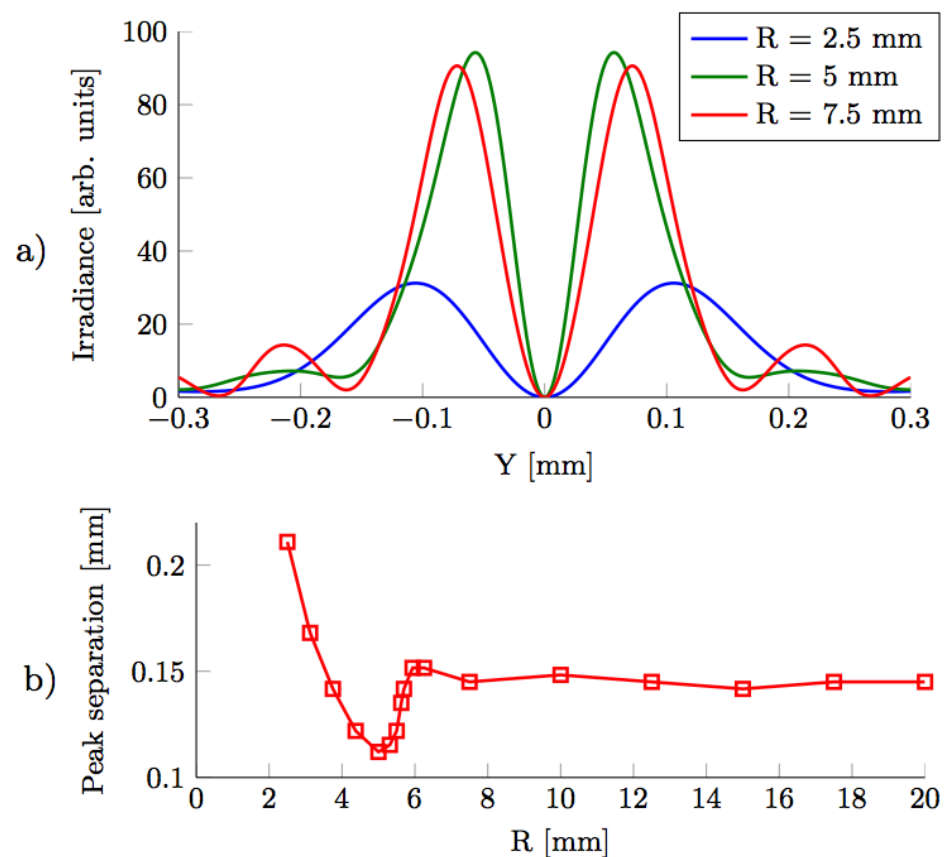
FIG. 7. TR PSF (a) and distance between the two main lobes (b) for various lens radii R ($\lambda = 550$ nm, $\gamma = 2500$, $\theta_x = 0$, $M = -10$).

OTR PSF – realistic beam sizes

OTR irradiance X-Cross section at the image plane for γ=2500

Legend: λ=500nm, λ=550nm, λ=600nm, λ=700nm

Irradiance [Watts/mm^2] vs Y coordinate [μm]
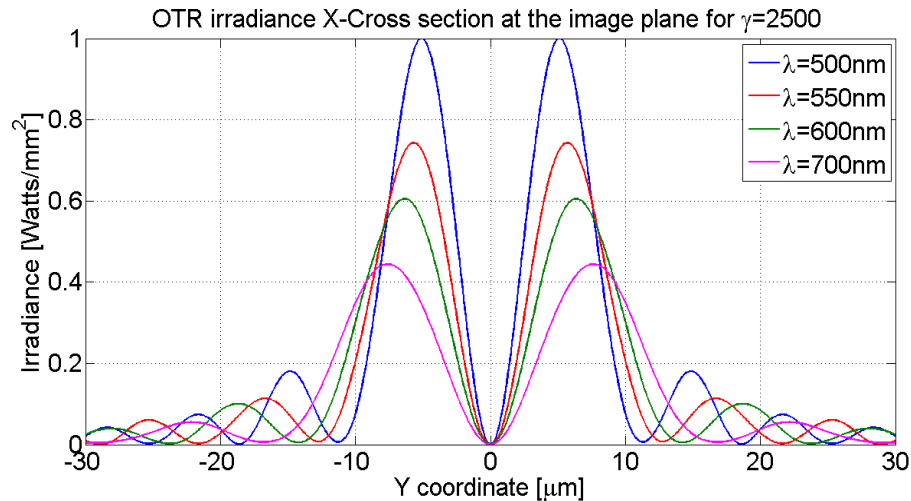
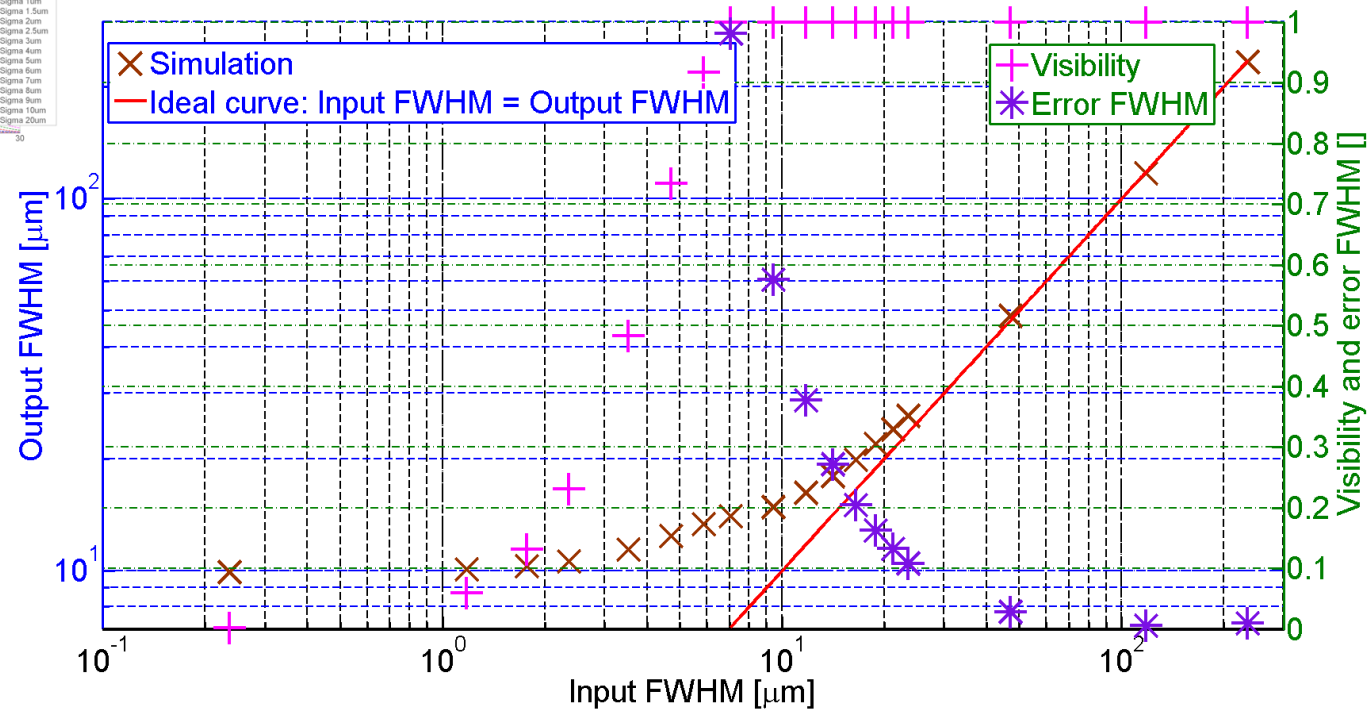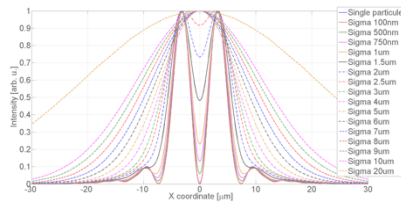1. Point Spread Function of OTR imaging system: Image generated by a single particle (propagating the OTR E-field in Zemax)

$$\Re\{E_y\} = \frac{2e}{\gamma\lambda\cos\theta_0}\left\{\frac{y}{\rho}K_1\left[\frac{2\pi}{\beta\gamma\lambda}\rho\right]\cos\phi\cos\theta_0\right. \quad (1)$$
$$\left.+\frac{1}{\gamma}K_0\left[\frac{2\pi}{\beta\gamma\lambda}\rho\right]\sin\phi\sin\theta_0\right\}$$

$$\Im\{E_y\} = \frac{2e}{\gamma\lambda\cos\theta_0}\left\{\frac{y}{\rho}K_1\left[\frac{2\pi}{\beta\gamma\lambda}\rho\right]\sin\phi\cos\theta_0\right. \quad (2)$$
$$\left.-\frac{1}{\gamma}K_0\left[\frac{2\pi}{\beta\gamma\lambda}\rho\right]\cos\phi\sin\theta_0\right\},$$

with $\beta = \sqrt{1-\frac{1}{\gamma^2}}$, phase shift $\phi = ky\tan\theta_0\left(1-\frac{1}{\beta}\right)$, $k = \frac{2\pi}{\lambda}$ and $\rho = \sqrt{x^2+y^2}$

2. Simulation of images obtained for realistic beam size: **Sub-micron beam sizes can be measured via the visibility of the PSF**

Intensity [arb. u.] vs X coordinate [μm]

Legend: Single particule, Sigma 100nm, Sigma 500nm, Sigma 750nm, Sigma 1um, Sigma 1.5um, Sigma 2um, Sigma 2.5um, Sigma 3um, Sigma 4um, Sigma 5um, Sigma 6um, Sigma 7um, Sigma 8um, Sigma 9um, Sigma 10um, Sigma 20um
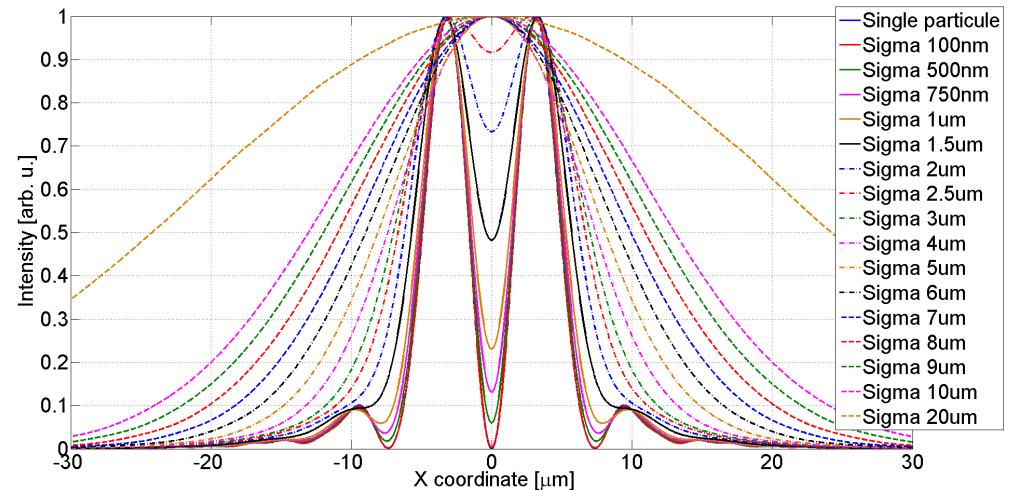
Estimation of systematic errors using OTR imaging system

1. Using PSF visibility: beam size extraction with FWHM from 1.2 to 6µm
2. Fit with large errors (≈100%) for input beam size just larger than 6µm FWHM (with the PSF having FWHM of 10µm)
3. For larger beam sizes error becomes smaller and smaller

ODR – circular aperture

Charged particle moving normally through the centre of a circular hole in an infinitely thin, perfectly conducting disc [4]

$$E_y(\mathbf{r}, \omega) = \frac{ie}{\pi\gamma} \frac{F(b) - F(a)}{\gamma^{-2} + \theta_x{}^2 + \theta_y{}^2}$$

$$F(a) = ak\theta J_0(ak\theta) K_1\left(\frac{a\omega}{v\gamma}\right) + \frac{a\omega}{v\gamma} J_1(ak\theta) K_0\left(\frac{a\omega}{v\gamma}\right)$$

$$\frac{d^2 W_y^{hole}}{d\omega d\Omega} = 4\pi^2 |E_y|^2$$

[4] A. P. Potylitsyn et al., Springer Tracts Mod. Phys. 239, 1 (2011).

incident field radius

hole radius
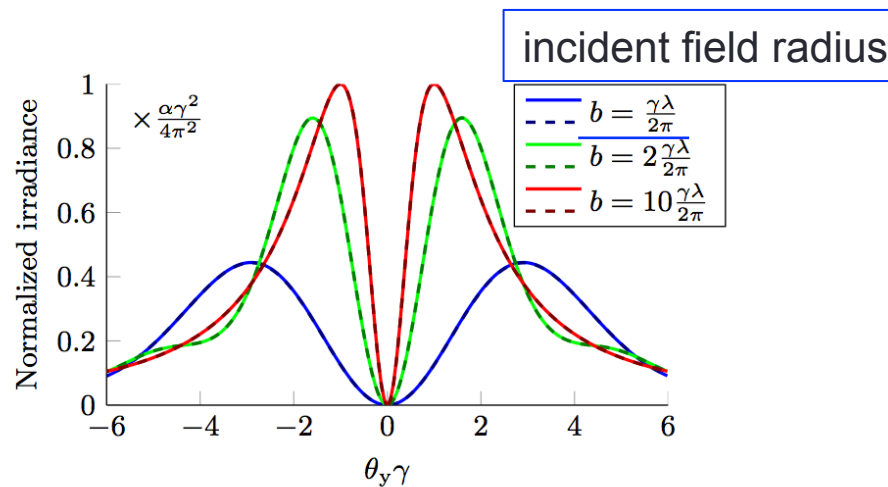
FIG. 8. Comparison between theoretical (dashed) and simulated (solid) DR angular distribution in the far-field for various target disc radii b ($\lambda = 400$ nm, $\gamma = 4110$, $\theta_x = 0$, $a = 1$ nm).

infinitely small hole
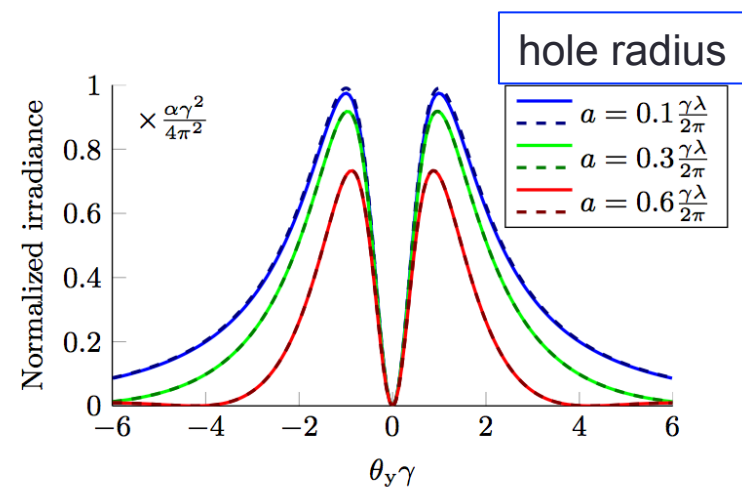
FIG. 9. Comparison between theoretical (dashed) and simulated (solid) DR angular distribution in the far-field for various hole radii a ($\lambda = 400$ nm, $\gamma = 4110$, $\theta_x = 0$, $b = 10\frac{\gamma\lambda}{2\pi}$).

infinite target

ODR – circular aperture – target tilt

- Asymmetry for low beam energies: increasing asymmetry of the angular distribution for large tilt angles.
- Increase in overall intensity: from the decrease in effective hole diameter in the projection onto the source plane.
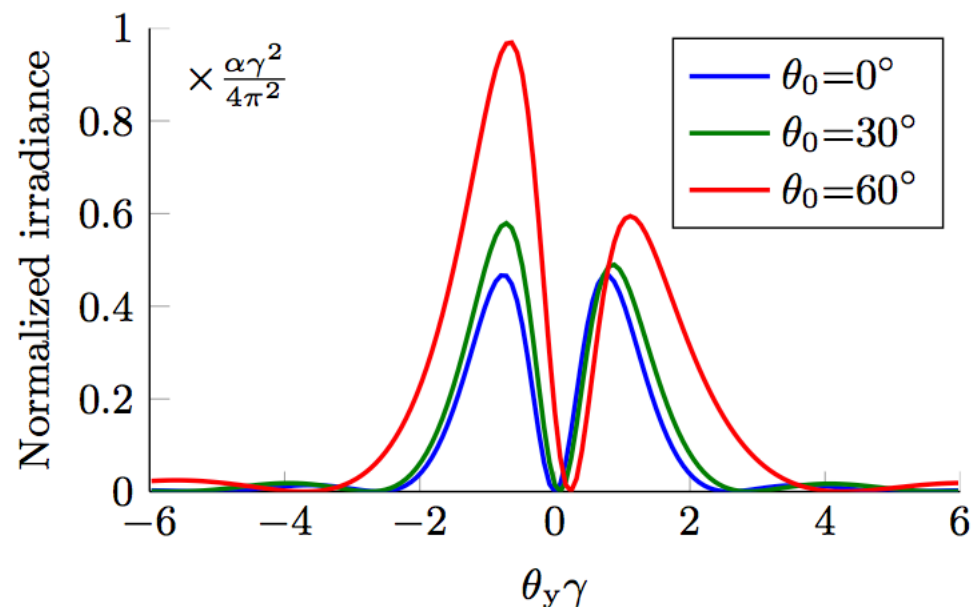
FIG. 10. DR angular distribution in the far-field for various tilt angles θ_0 ($\lambda = 400$ nm, $\gamma = 10$, $\theta_x = 0$, $a = \frac{\gamma\lambda}{2\pi}$, $b = 10\frac{\gamma\lambda}{2\pi}$).

ODR – circular aperture – beam offset
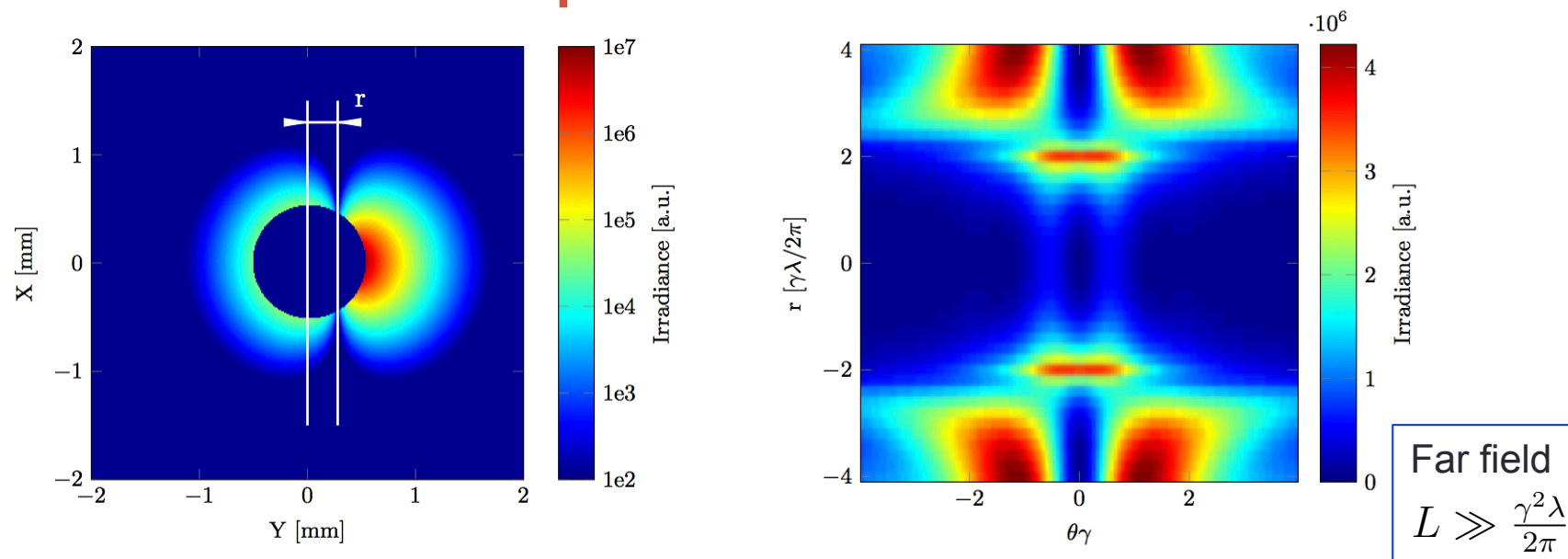
FIG. 10. Electric field at the source for single electron passing through circular hole with a beam offset of $r = \frac{\gamma\lambda}{2\pi}$ ($\lambda = 400$ nm, $\gamma = 4110$, $a = 2\frac{\gamma\lambda}{2\pi}$).

FIG. 11. DR angular distribution in the far-field for various beam offsets r ($\lambda = 400$ nm, $\gamma = 4110$, $a = 2\frac{\gamma\lambda}{2\pi}$, $L = 100\frac{\gamma^2\lambda}{2\pi}$).

Far field

$$L \gg \frac{\gamma^2\lambda}{2\pi}$$

Each horizontal line represents the cross-section of the angular distribution for a beam of a certain offset. Starting with a beam offset of $r = -4\gamma\lambda/2\pi$, the distribution is almost pure TR. The closer the beam moves to the centre of the hole, the more DR like the distribution becomes. When moving the beam up even more, TR is established again for a beam offset of $r = 4\gamma\lambda/2\pi$.

ODR – circular aperture – beam offset
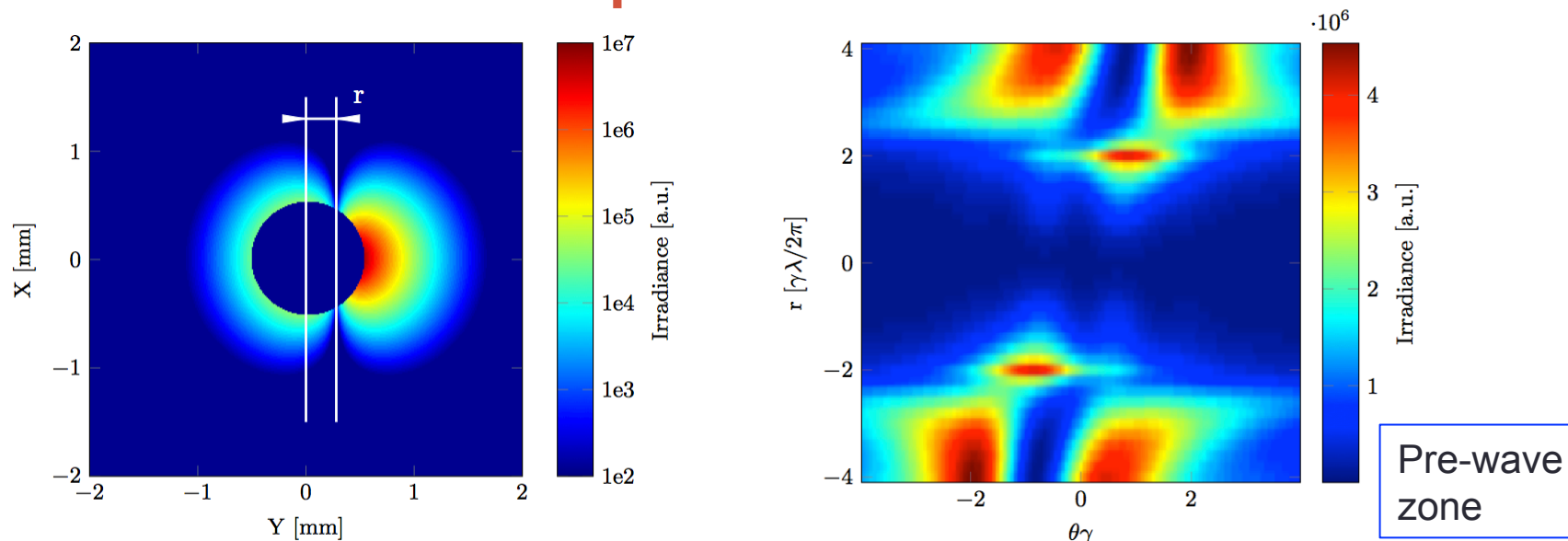
FIG. 10. Electric field at the source for single electron passing through circular hole with a beam offset of $r = \frac{\gamma\lambda}{2\pi}$ ($\lambda = 400$ nm, $\gamma = 4110$, $a = 2\frac{\gamma\lambda}{2\pi}$).

FIG. 12. DR angular distribution in the pre-wave zone for various beam offsets r ($\lambda = 400$ nm, $\gamma = 4110$, $a = 2\frac{\gamma\lambda}{2\pi}$, $L = 5\frac{\gamma^2\lambda}{2\pi}$).

Pre-wave zone

In the pre-wave zone an asymmetry can be found. This originates from the interference of the radiation from different parts of the target.

ODR – slit aperture

- Charged particle moving through a slit between two tilted semi-planes i.e. only DR produced from the target is considered. The vertical polarisation component is sensitive to beam size. ODR vertical polarisation component convoluted with a Gaussian distribution [2]:

$$\frac{d^2 W_y^{slit}}{d\omega d\Omega} = \frac{\alpha \gamma^2}{2\pi^2} \frac{\exp\left(-\frac{2\pi a}{\gamma \lambda \cos\theta_0}\sqrt{1+t_x^2}\right)}{1+t_x^2+t_y^2} \left\{ \exp\left[\frac{8\pi^2 \sigma_y^2}{\lambda^2 \gamma^2}\left(1+t_x^2\right)\right]\cosh\left(\frac{4\pi \bar{a}_x}{\gamma\lambda}\sqrt{1+t_x^2}\right) - \cos\left(\frac{2\pi a}{\gamma\lambda\cos\theta_0}t_y+2\psi\right) \right\}$$

  with $t_{x,y}=\gamma\theta_{x,y}$ and ψ=arctan($t_y/(1+t_x^2)$). Valid when the transition radiation contribution from the tails of the Gaussian distribution is negligible (approx. a ≥ $4\sigma_y$).

- For slit width a=0 (and a_x=0, σ_y=0) → OTR

[2] P. Karataev et al., Phys. Rev. Lett. 93 (2004) 244802.

ODR – slit aperture – pre-wave zone

- To obtain the DR angular distribution in the pre-wave zone, a focusing lens with the detector positioned in the back focal plane is used to remove the spatial contribution
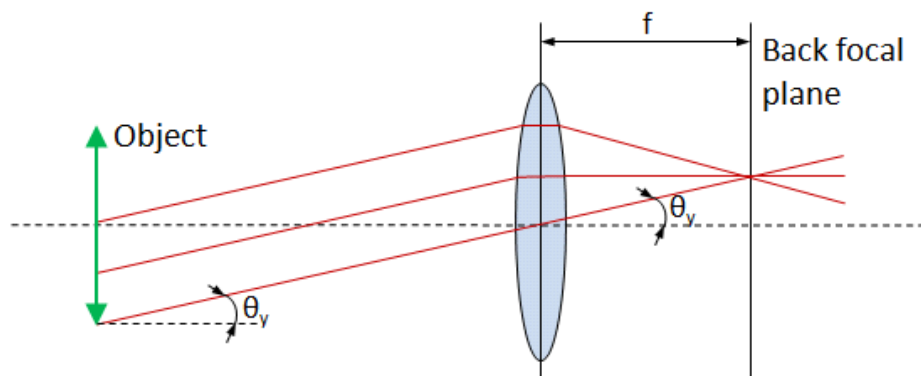
- Far-field
- Pre-wave zone using an ideal paraxial lens with a focal length of f=500mm
- Pre-wave zone with a plano-convex Thorlabs LA4782-UV lens (f = 500 mm, Ø50.8 mm) → CesrTA
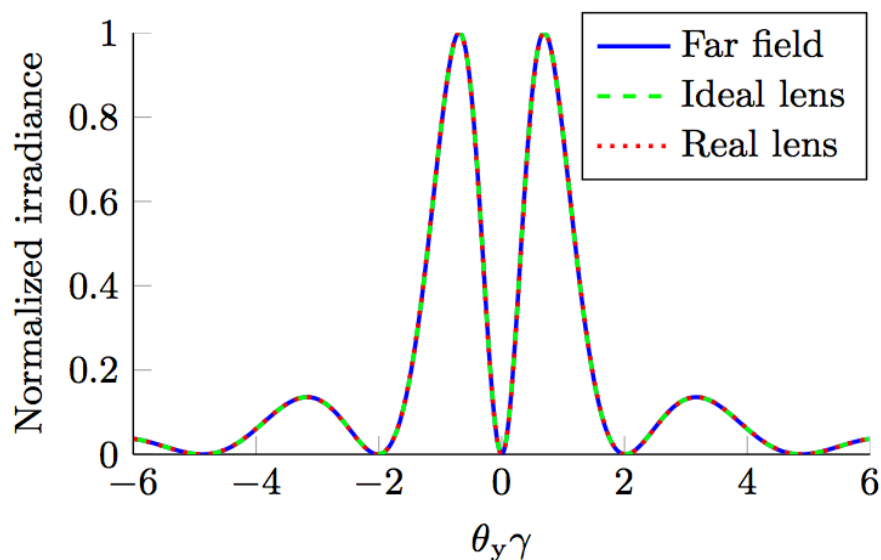
FIG. 15. Comparison of the DR angular distribution in the far-field, in the back focal plane of an ideal lens and in the back focal plane of the plano-convex lens ($\lambda = 400$ nm, $\gamma = 4110$, $\theta_x = 0$, $a = \frac{\gamma \lambda}{2\pi}$).

ODR – slit aperture – misalignments

- Very serious distortion of the ODR angular distribution occurs at large lens tilt angles, but accuracy much better than 10° can easily be achieved.
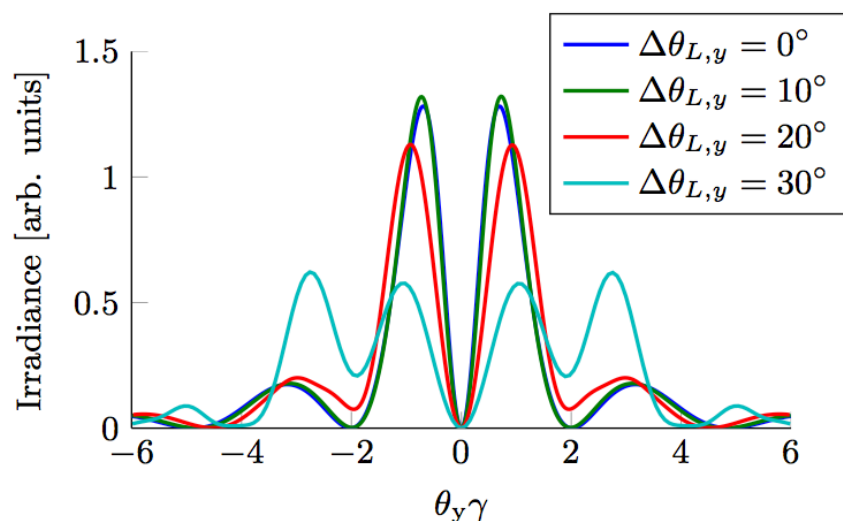
FIG. 16. DR angular distribution in the back focal plane of the plano-convex lens for various vertical lens tilts $\Delta\theta_{L,y}$ ($\lambda = 400$ nm, $\gamma = 4110$, $\theta_x = 0$, $a = \frac{\gamma\lambda}{2\pi}$).
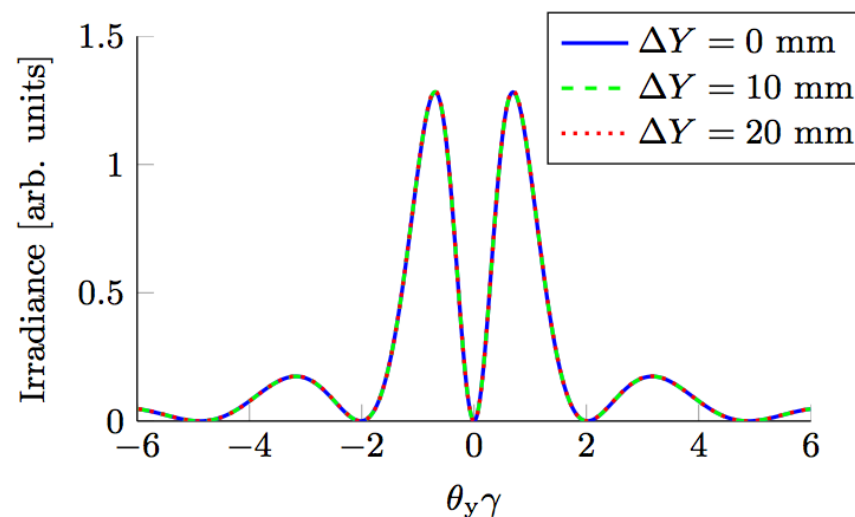
FIG. 17. DR angular distribution in the back focal plane of the plano-convex lens for various vertical lens offsets ΔY ($\lambda = 400$ nm, $\gamma = 4110$, $\theta_x = 0$, $a = \frac{\gamma\lambda}{2\pi}$).

- BUT barely any distortion in the distribution pattern can be observed, even for large lens offsets.

ODR – arbitrary aperture

- Can also simulate the vertical polarization component of the DR angular distribution using a target with arbitrarily shaped aperture.
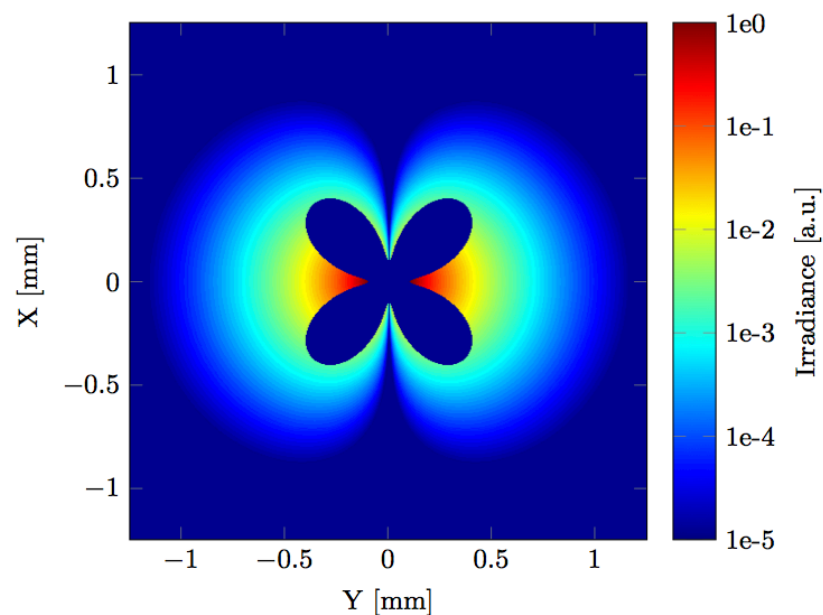
FIG. 17. Vertically polarised electric field at the source for a four-leafed aperture ($\lambda = 400$ nm, $\gamma = 4110$, $a = 2\frac{\gamma\lambda}{2\pi}$).
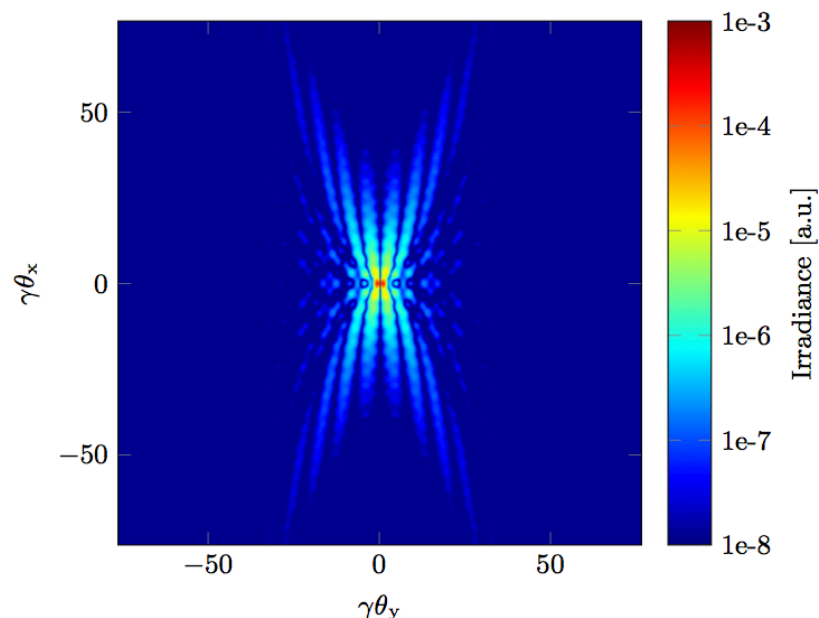
FIG. 18. DR angular distribution vertical polarisation for a four-leafed aperture in the far-field ($\lambda = 400$ nm, $\gamma = 4110$, $a = 2\frac{\gamma\lambda}{2\pi}$, $L = 10\frac{\gamma^2\lambda}{2\pi}$).

Hi-res beam size monitor using OTR PSF visibility

ATF2 OTR @ KEK in 2013

Interaction Chamber

QM14FF

e- beam

OTR

QM13FF

Motorized mirror
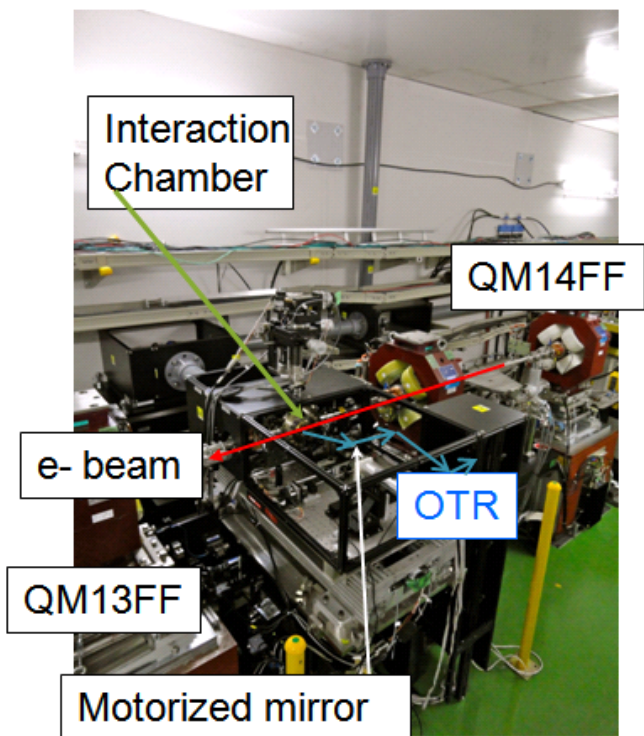
Installed optical system designed using Zemax simulations

Vertical projection

I_{max}

I_{min}
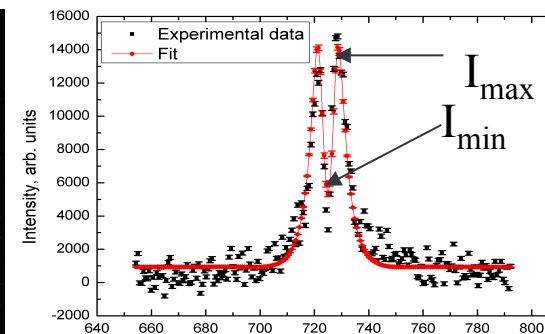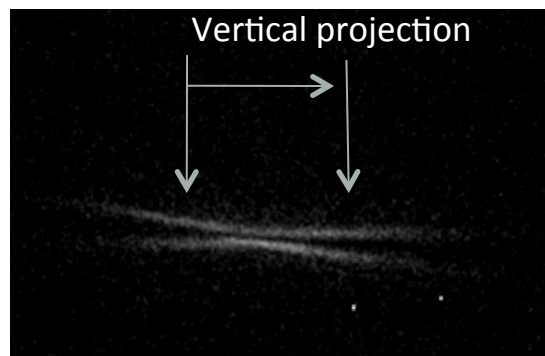
PSF-like fit function:

$$f(x) = a_0 + \frac{a_1\left(a_4 + (x - a_3)^2\right)}{1 + \left(a_2\left(x - a_3\right)\right)^4}$$

Minimum measured beam size of 0.754±0.034μm
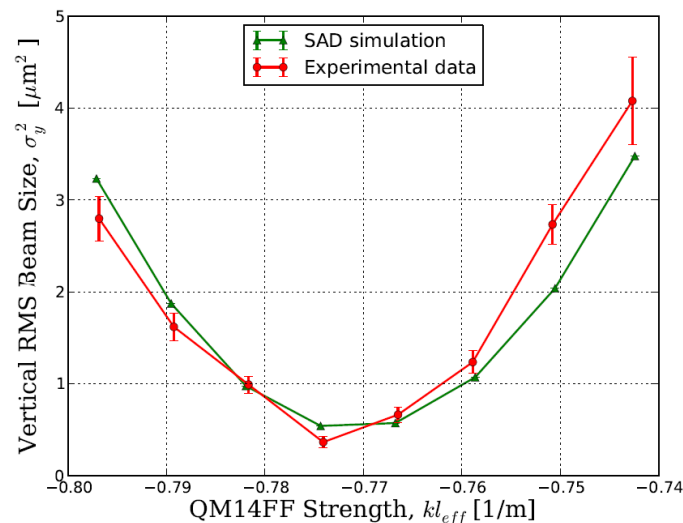
Comparison of experimental results with Zemax simulations
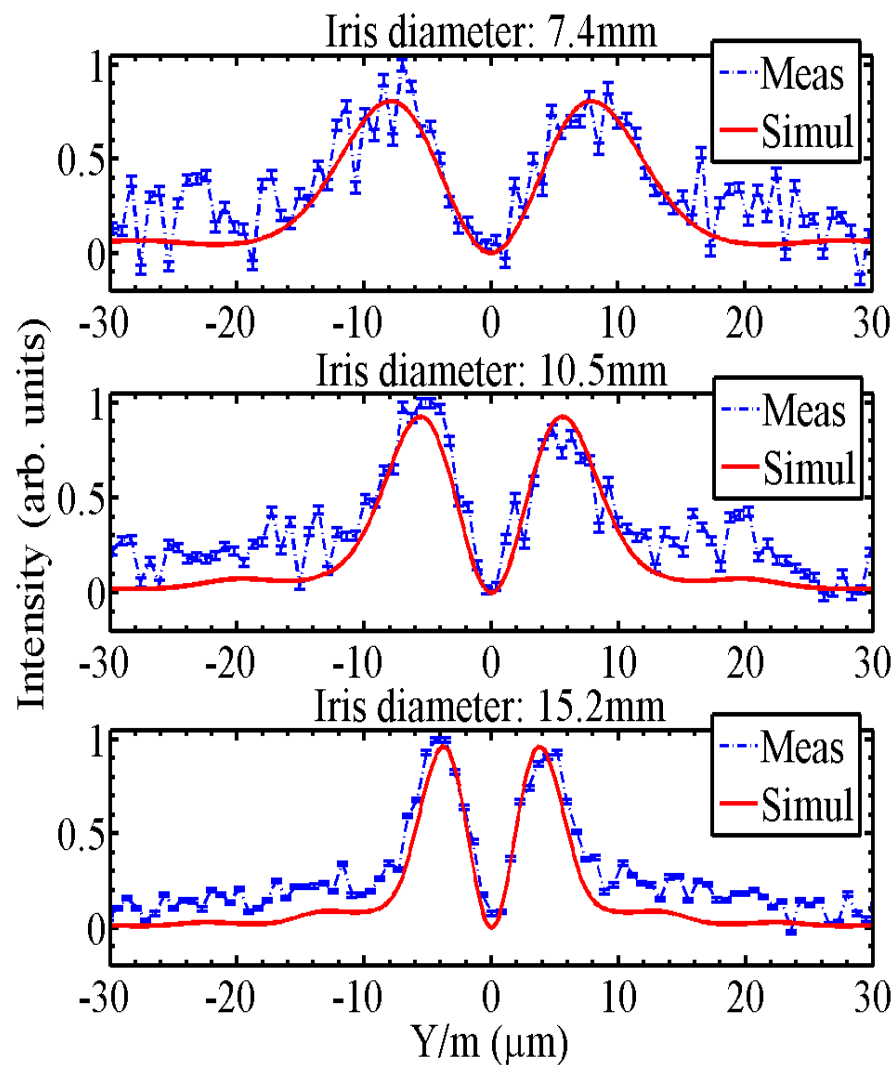
Investigation of the diffraction effect:

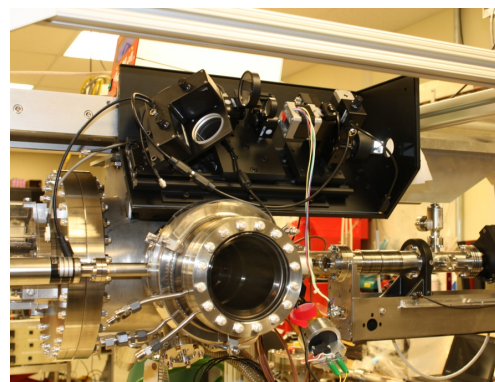OTR PSF size (distance between peaks and FWHM) for different iris diameters
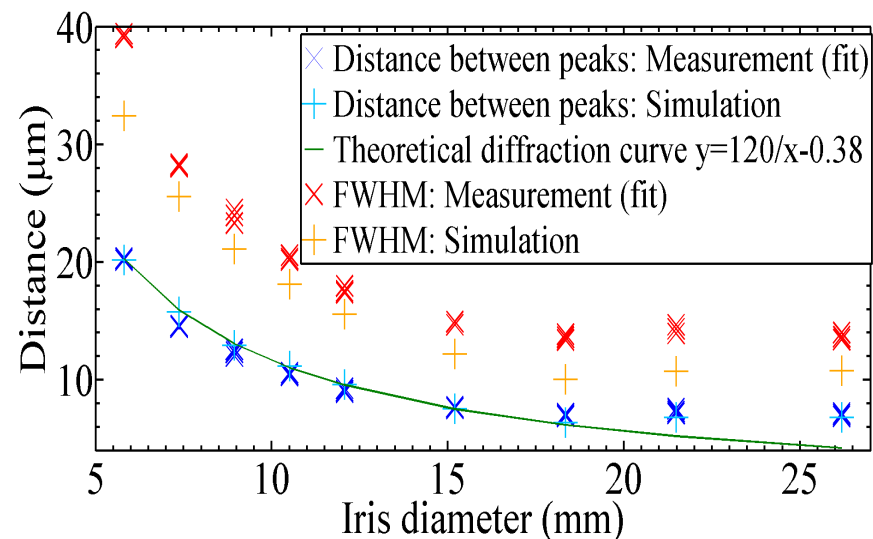
ODR development: non-invasive beam size measurements using DR from slit
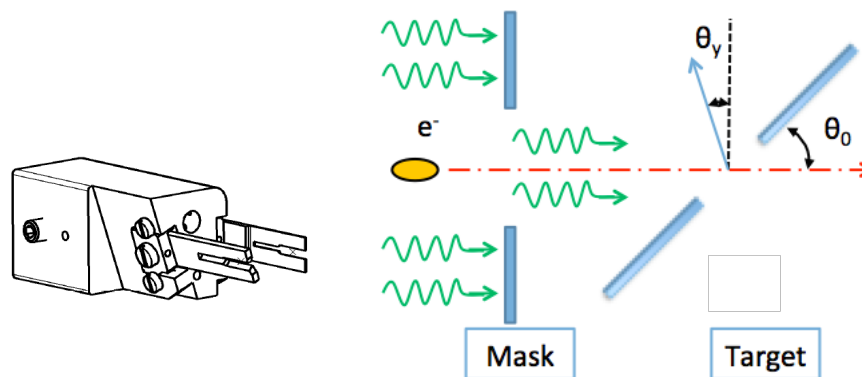
1. Simulation using Zemax

Single particle images
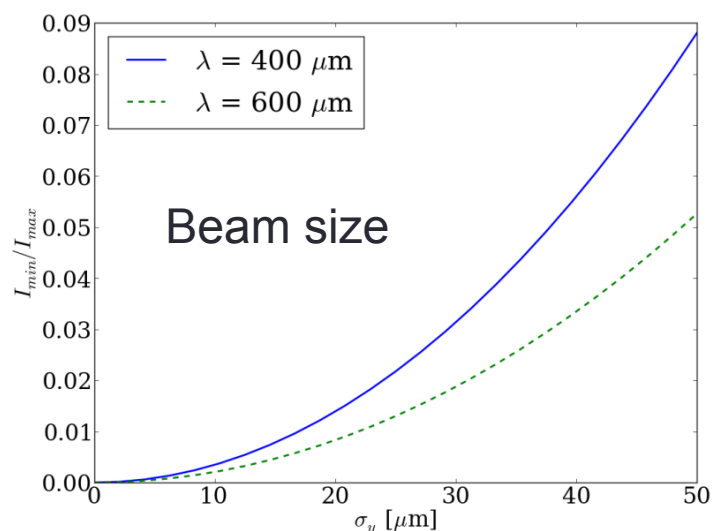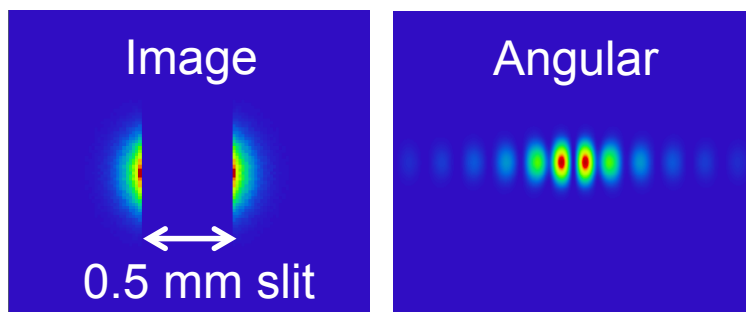
0.5 mm slit

2. Beam tests at Cornell Electron Storage Ring since Dec 2012
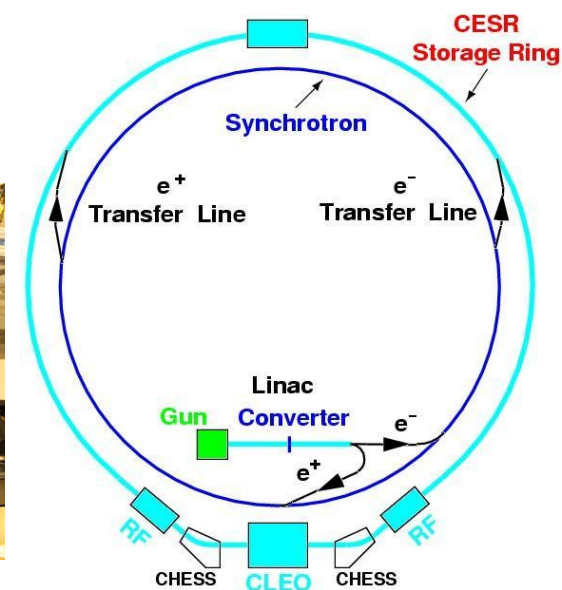
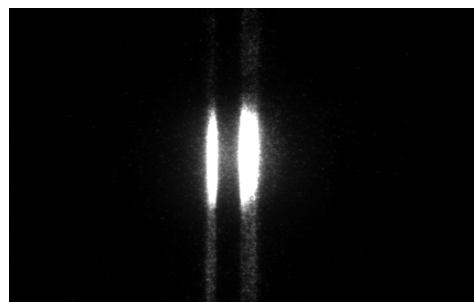| E [GeV]	σ_H [µm]	σ_V [µm]
2.1	320	10

ODR target slit

Target Assembly

- Si target for DR
  - Ultra high precision: 0.1nm roughness, 40nm co-planarity
  - Slit size: 0.5mm
- SiC mask to suppress background from synchrotron radiation
  - Mask aperture of 1 and 2 mm
  - Small mask aperture leads to stronger interference between the DR of the mask and target
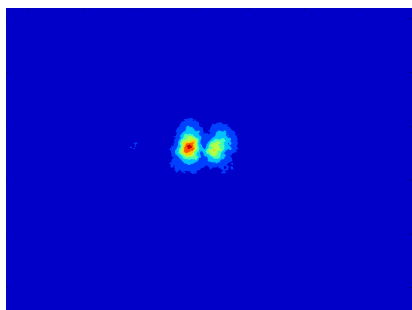
Target imaging at 600nm
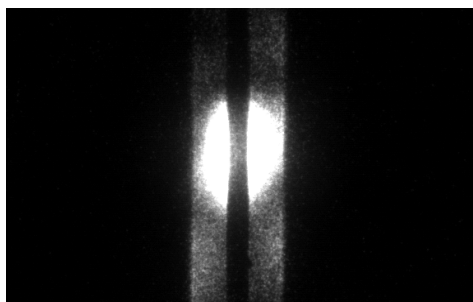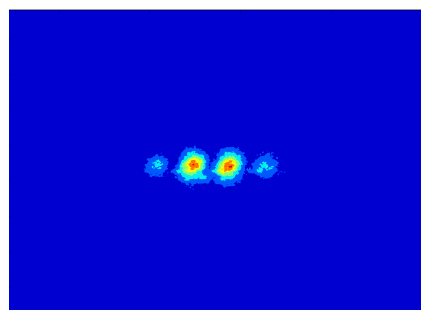
2mm mask aperture   1mm mask aperture

Asymmetry in the distribution indicates a beam position offset in the slit

ODR @CESR-TA: data analysis
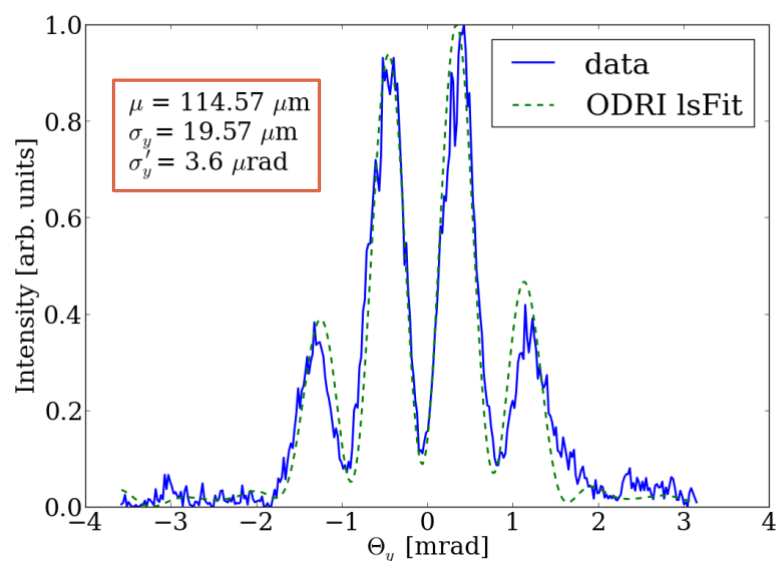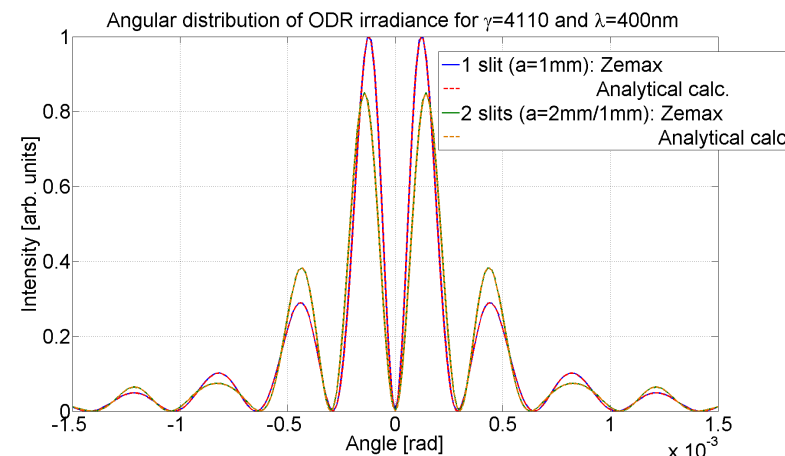
Angular distribution at 600nm

2mm mask, ODR   1mm mask, ODRI

Zemax simulation ODR/ODRI

Least Square Fit Analysis

Taking into account target co-planarity of 40nm
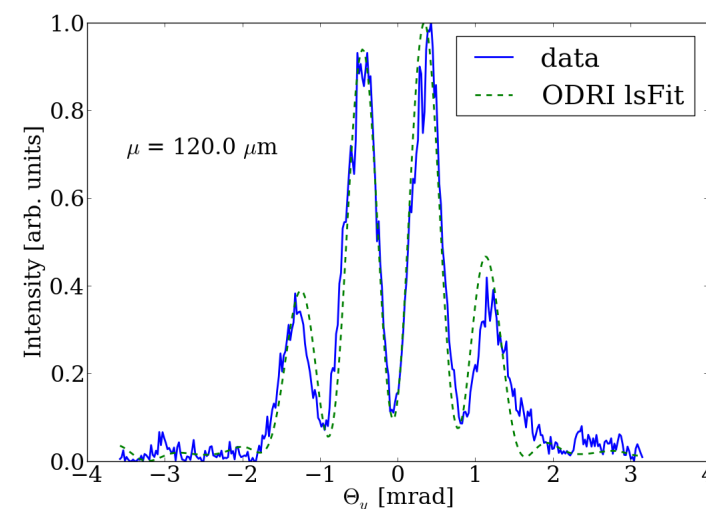
3 fit parameters: position, size and divergence

CESR measured beam parameters

ε_y [m]	σ_y (ODR) [µm]	σ_y' (ODR) [µrad]
3.96e-11	17.6	4.08

Conclusions

- With assumptions similar to theoretical boundary conditions, Zemax simulations of TR and DR agree with the analytical expressions.

- Off-axis incident field or an arbitrarily shaped aperture does not slow down the Zemax simulations noticeably; it is therefore the preferable method.

- Finite beam size: displacing the single particle with respect to the optical axis across the transversal profile → angular pattern for each step can then be weighted and summed up.

- This tool represents the most comprehensive approach to the design of a real diagnostics based on either OTR or ODR including all misalignment errors (shifts, tilts) and optimisation of a real optical system (including viewports, polarisers, filters, etc.).

- Simulations are now fully predictive – match theory and measurements

ANY QUESTIONS?

Thank you for your attention!